Brain Advance Access published October 17, 2011

BRAIN
A JOURNAL OF NEUROLOGY

Functional connectivity magnetic resonance imaging classification of autism

Jeffrey S. Anderson,[1,2,3,4] Jared A. Nielsen,[2,5] Alyson L. Froehlich,[5] Molly B. DuBray,[2,5] T. Jason Druzgal,[6] Annahir N. Cariello,[5] Jason R. Cooperrider,[2,5] Brandon A. Zielinski,[7,8] Caitlin Ravichandran,[9,10,11] P. Thomas Fletcher,[3,12,13] Andrew L. Alexander,[14,15] Erin D. Bigler,[3,16] Nicholas Lange[9,10,11] and Janet E. Lainhart[2,3,5]

1 Division of Neuroradiology, University of Utah, Salt Lake City, UT 84112, USA
2 Interdepartmental Program in Neuroscience, University of Utah, Salt Lake City, UT 84112, USA
3 The Brain Institute at the University of Utah, Salt Lake City, UT 84112, USA
4 Department of Bioengineering, University of Utah, Salt Lake City, UT 84112, USA
5 Department of Psychiatry, University of Utah, Salt Lake City, UT 84112, USA
6 Department of Radiology, University of Virginia, Charlottesville, VA 22908, USA
7 Department of Paediatrics, University of Utah, Salt Lake City, UT 84112, USA
8 Division of Child Neurology, University of Utah, Salt Lake City, UT 84112, USA
9 Neurostatistics Laboratory, McLean Hospital, Belmont, MA 02478, USA
10 Department of Psychiatry, Harvard School of Public Health, Boston, MA 02115, USA
11 Department of Biostatistics, Harvard School of Public Health, Boston, MA 02115, USA
12 School of Computing, University of Utah, Salt Lake City, UT 84112, USA
13 Scientific Computing and Imaging Institute, University of Utah, Salt Lake City, UT 84112, USA
14 Department of Medical Physics, Waisman Laboratory for Brain Imaging and Behaviour, Waisman Centre, University of Wisconsin-Madison, Madison, WI 53705, USA
15 Department of Psychiatry, Waisman Laboratory for Brain Imaging and Behaviour, Waisman Centre, University of Wisconsin-Madison, Madison, WI 53705, USA
16 Department of Psychology and Neuroscience Centre, Brigham Young University, Provo, UT 84602, USA

Correspondence to: Jeffrey S. Anderson,
Department of Neuroradiology,
University of Utah,
1A71 School of Medicine,
Salt Lake City, UT 84132, USA
E-mail: andersonjeffs@gmail.com

Group differences in resting state functional magnetic resonance imaging connectivity between individuals with autism and typically developing controls have been widely replicated for a small number of discrete brain regions, yet the whole-brain distribution of connectivity abnormalities in autism is not well characterized. It is also unclear whether functional connectivity is sufficiently robust to be used as a diagnostic or prognostic metric in individual patients with autism. We obtained pairwise functional connectivity measurements from a lattice of 7266 regions of interest covering the entire grey matter (26.4 million connections) in a well-characterized set of 40 male adolescents and young adults with autism and 40 age-, sex- and IQ-matched typically developing subjects. A single resting state blood oxygen level-dependent scan of 8 min was used for the classification in each subject. A leave-one-out classifier successfully distinguished autism from control subjects with 83% sensitivity and 75% specificity for a total accuracy of 79% ($P = 1.1 \times 10^{-7}$). In subjects <20 years of age, the classifier performed at 89% accuracy ($P = 5.4 \times 10^{-7}$). In a replication dataset consisting of 21 individuals from six families with both affected and unaffected siblings, the classifier performed at 71% accuracy (91% accuracy for subjects <20 years of age). Classification scores in

Received May 4, 2011. Revised July 28, 2011. Accepted July 29, 2011.

subjects with autism were significantly correlated with the Social Responsiveness Scale ($P = 0.05$), verbal IQ ($P = 0.02$) and the Autism Diagnostic Observation Schedule-Generic's combined social and communication subscores ($P = 0.05$). An analysis of informative connections demonstrated that region of interest pairs with strongest correlation values were most abnormal in autism. Negatively correlated region of interest pairs showed higher correlation in autism (less anticorrelation), possibly representing weaker inhibitory connections, particularly for long connections (Euclidean distance >10 cm). Brain regions showing greatest differences included regions of the default mode network, superior parietal lobule, fusiform gyrus and anterior insula. Overall, classification accuracy was better for younger subjects, with differences between autism and control subjects diminishing after 19 years of age. Classification scores of unaffected siblings of individuals with autism were more similar to those of the control subjects than to those of the subjects with autism. These findings indicate feasibility of a functional connectivity magnetic resonance imaging diagnostic assay for autism.

Keywords: autism spectrum disorders; resting state functional MRI; brain development; functional MRI; functional connectivity MRI

Abbreviations: ADI-R = Autism Diagnostic Interview-Revised; ADOS-G = Autism Diagnostic Observation Schedule-Generic; BOLD = blood oxygen level-dependent

Introduction

One of the most replicated abnormalities in brain imaging studies of autism has been underconnectivity of distributed brain networks (Brock *et al.*, 2002; Belmonte *et al.*, 2004*a*, *b*; Just *et al.*, 2004; Courchesne and Pierce, 2005; Geschwind and Levitt, 2007; Hughes, 2007; Casanova and Trippe, 2009; Muller *et al.*, 2011). Most reports of underconnectivity in autism have focused on specific brain regions or networks, including regions underlying language (Just *et al.*, 2004; Kana *et al.*, 2006; Jones *et al.*, 2010), working memory (Koshino *et al.*, 2005, 2008; Kana *et al.*, 2007), motor function (Mostofsky *et al.*, 2009), theory of mind (Mason *et al.*, 2008), executive function (Just *et al.*, 2007), long-range anterior–posterior connections (Cherkassky *et al.*, 2006; Kana *et al.*, 2009), interhemispheric connections (Anderson *et al.*, 2011*b*; Dinstein *et al.*, 2011), visual attention (Belmonte *et al.*, 2010), the default mode network (Kennedy *et al.*, 2006; Kennedy and Courchesne, 2008*a*, *b*; Lombardo *et al.*, 2009; Monk *et al.*, 2009; Weng *et al.*, 2009; Assaf *et al.*, 2010), response inhibition (Lee *et al.*, 2009), visuospatial function (Villalobos *et al.*, 2005; Damarla *et al.*, 2010), corticostriatal connections (Di Martino *et al.*, 2008, 2009) and facial recognition (Kleinhans *et al.*, 2008; Koshino *et al.*, 2008). The underlying hypothesis supported by these studies is a theory of connectivity characterized by local over-connectivity but long-distance underconnectivity in autism (Just *et al.*, 2004; Courchesne and Pierce, 2005; Geschwind and Levitt, 2007; Rippon *et al.*, 2007; Casanova and Trippe, 2009).

Abnormal brain connectivity in autism occurs in a context of white matter microstructural abnormalities and neuropathological changes that are consistent with disordered connectivity. Increased cellular density in cortical minicolumns with reduced lateral inhibition (Casanova *et al.*, 2009; Casanova and Trippe, 2009) and abnormal white matter anisotropy in diffusion tensor imaging studies (Alexander *et al.*, 2007; Brito *et al.*, 2009; Cheung *et al.*, 2009; Fletcher *et al.*, 2010; Lange *et al.*, 2010; Shukla *et al.*, 2010, 2011) are both consistent with abnormal density and arborization of white matter projection fibres in autism.

Yet, despite extensive evidence that autism is in some fundamental way a disorder of brain connectivity, a cohesive framework for describing the distribution of connectivity abnormalities is lacking (Muller *et al.*, 2011). It remains unclear whether connectivity disturbances involve preferentially specific brain regions or tract lengths, the extent to which excitatory and inhibitory connections are involved, at what ages in development disturbances arise or may normalize and whether connectivity abnormalities are related to the heterogeneous functional deficits in autism spectrum patients.

The extent to which single-subject connectivity measurements may assist in clinical diagnosis, given the well-characterized noise in functional connectivity measurements, is also unclear. Test–retest studies have shown limited reproducibility that improves with increased imaging time (Shehzad *et al.*, 2009; Zuo *et al.*, 2009; Van Dijk *et al.*, 2010; Anderson *et al.*, 2011*d*). Despite these apparent limitations, useful diagnostic information has been obtained from even short blood oxygen level-dependent (BOLD) sequences, such as characterization of subject age (Dosenbach *et al.*, 2010) and classification of dementia (Chen *et al.*, 2011). In this study, we used a data-driven approach to characterize whole-brain functional connectivity abnormalities in a dataset of adolescents and young adults with autism and typically developing controls, and to determine whether these abnormalities could accurately classify individual subjects with autism.

Materials and methods

Participant selection

Training sample

Forty high-functioning adolescent and young adult males with autism were compared with 40 male typically developing control volunteers, group-matched by age and performance IQ. Subjects were selected from a sample of 53 subjects with autism and 43 typically developing control subjects by selecting the subset of autism subjects with highest performance IQ, and control subjects with lowest performance IQ in the sample. The participants had no history of hearing problems; all had English as their first language. Subject characteristics are displayed in Table 1.

Table 1 Characterization of control ($n = 40$ in training sample and $n = 13$ in the replication sample) and autism ($n = 40$ in the training sample and $n = 8$ in the replication sample) populations

	Autism		Control		*P*
	n	Mean (SD) (range)	*n*	Mean (SD) (range)	
Training sample					
Gender	40 males		40 males		
Age	40	22.7 (7.4) (12 to 42)	40	21.6 (7.4) (8 to 39)	0.49
EHI	40	58.2 (53.4) (−93 to 100)	39	71.2 (28.3) (−27 to 100)	0.18
VIQ	40	107.9 (18.9) (63 to 139)	40	113.5 (12.7) (90 to 140)	0.13
PIQ	40	106.2 (13.6) (81 to 133)	40	111.8 12.1 (88 to 135)	0.06
SRS	39	97.3 (31.0) (26 to 151)	39	13.6 (11.6) (0 to 51)	1.1E-25
ADOS S + C	39	12.8 (3.8) (6 to 21)	35	1.0 (1.27) (0 to 4)	1.0E-26
ADI-R Soc	38	19.0 (6.7) (9 to 39)			
ADI-R Com	38	14.0 (4.8) (6 to 24)			
ADI-R RSB	38	6.9 (2.3) (2 to 12)			
Replication sample					
Gender	6 males, 2 females		6 males, 7 females		
Age	8	16.1 (3.6) (11 to 22)	13	20.8 (8.0) (7 to 32)	
EHI					
VIQ	6	88.8 (21.1) (60 to 113)	12	108.1 (14.7) (75 to 126)	
PIQ	6	93.8 (17.6) (64 to 112)	12	113.4 (15.2) (89 to 135)	
SRS	2	66.5 (3.5) (64 to 69)	13	16.0 (11.7) (3 to 45)	
ADOS S + C	7	11.0 (4.8) (5 to 18)			
ADI-R Soc	7	18.0 (6.1) (11 to 28)			
ADI-R Com	7	14.0 (7.0) (5 to 24)			
ADI-R RSB	7	5.0 (1.7) (2 to 7)			

EHI = Edinburgh Handedness Inventory; PIQ = performance IQ; SRS = Social Responsiveness Scale; VIQ = verbal IQ.

Replication sample

An additional 21 subjects from six families, each with at least one member with an autism spectrum disorder, which included eight individuals with an autism spectrum disorder and 13 siblings without an autism spectrum disorder, were examined. The sample included nine females and 12 males ranging in age from 7 to 32 years of age. Three subjects that could have potentially been included in the replication sample were excluded because they were already included in the training sample.

All experiments were undertaken with the understanding and written consent of each subject, with the approval of the University of Utah Institutional Review Board, and in compliance with the national legislation and the Code of Ethical Principles for Medical Research Involving Human Subjects of the World Medical Association.

Diagnosis and exclusion criteria

Lifetime diagnosis of autism was established by the Autism Diagnostic Interview-Revised (ADI-R) (Lord *et al.*, 1994), Autism Diagnostic Observation Schedule-Generic (ADOS-G) (Lord *et al.*, 2000), DSM-IV (American Psychiatric Association, 1994) and ICD-10 criteria. The diagnosis was established by an autism expert (J.E.L.) using the ADOS-G and DSM-IV/ICD-10 criteria in two subjects and using the ADI-R and DSM-IV/ICD-10 criteria in one subject from the training sample. Six training sample subjects and two replication sample subjects met lifetime diagnostic criteria for pervasive developmental disorder not otherwise specified, and all others met diagnosis of autism. Individuals with medical causes of autism (identified by history, Fragile-X gene testing, karyotype and examination) were excluded.

Assessments

All participants underwent tests of IQ, language and neuropsychological function and were assessed with a standardized psychiatric interview (Leyfer *et al.*, 2006). Most controls were also assessed with the ADOS-G (Lord *et al.*, 2000) to confirm typical development. Four control subjects that were not assessed with the ADOS-G had Social Responsiveness Scale total scores <55 to confirm typical development (Duvall *et al.*, 2007). Controls with any history of developmental, learning, cognitive, neurological or neuropsychiatric conditions were excluded. One control subject reported a single minor bout of depression.

Handedness

The Edinburgh Handedness Inventory (Oldfield, 1971), a standardized assessment of hand preference, was obtained for each subject. This inventory consists of a numerical score between −100 and +100, where −100 represents strong left-handedness and +100 represents strong right-handedness.

IQ

Verbal IQ and performance IQ were measured with the Wechsler Adult Intelligence Scale, WAIS III ($n = 41$) (Wechsler, 1997), the Wechsler Intelligence Scale for Children, WISC III ($n = 4$) (Wechsler, 1991), the Wechsler Abbreviated Scale of Intelligence, WASI ($n = 6$)

(Wechsler, 1999) or the Differential Abilities Scale ($n = 29$) (Elliott, 1990).

Social function

The Social Responsiveness Scale is a standardized, quantitative, 65-item questionnaire with a four-point rating scale that measures social impairments characteristic of autism spectrum disorders (Constantino and Todd, 2003). Higher total raw scores indicate that the subject is less socially responsive.

Functional magnetic resonance imaging acquisition

Images were acquired on Siemens 3 Tesla Trio scanner. The scanning protocol consisted of initial 1 mm isotropic magnetization-prepared rapid acquisition with gradient echo (MPRAGE) acquisition for an anatomic template. BOLD echoplanar images (repetition time = 2.0 s, echo time = 28 ms, GRAPPA parallel acquisition with acceleration factor = 2, 40 slices at 3 mm slice thickness, 64×64 matrix) were obtained during the 8-min resting state scan (240 volumes), where subjects were instructed to 'Keep your eyes open and relax. Remain awake and try to let thoughts pass through your mind without focusing on anything in particular'. Prospective motion correction was performed during BOLD imaging.

Functional magnetic resonance imaging post-processing and statistical analysis

Offline post-processing was performed in MATLAB (Mathworks) using SPM8 (Wellcome Trust) software. Initial slice timing correction was performed to adjust for interleaved slice acquisition. A field map sequence was acquired for each subject for distortion correction, and all images were motion corrected using realign and unwarp procedures. There were no significant differences between the groups in head motion when maximal translational and maximal rotational head deviation was measured for each subject (two-tailed *t*-test: translational $P = 0.37$, rotational $P = 0.73$). BOLD images were coregistered to the MPRAGE anatomic image sequence for each subject. All images were normalized to the Montreal Neurological Institute (MNI) template brain (T1.nii in SPM8), with manual inspection of appropriate normalization in all subjects.

To correct for BOLD signal attributable to physiological noise such as heart rate and respiration, we used a regression algorithm using time series from voxels in the facial soft tissues, CSF and white matter to correct for artefactual correlations in the BOLD data (Fox *et al.*, 2009). No global signal regression was performed, to avoid introducing artefactual anticorrelations in the data (Murphy *et al.*, 2009; Anderson *et al.*, 2011*c*).

Scalp and facial soft tissues, CSF and white matter signal regression was performed after automated grey matter, white matter and CSF segmentation of each subject's MPRAGE volume using SPM8. These segmented images were inspected manually to confirm appropriate identification of tissue components. The CSF time series for each subject was measured from the lateral ventricles. This was obtained from selecting voxels from the CSF segmented image for each subject within the bounding box defined by MNI coordinates: $-35 < x < 35$, $-60 < y < 30$, $0 < z < 30$. White matter time series for each subject were obtained from the mean time series of voxels within two regions of interest in the bilateral centrum semiovale (MNI coordinates: *left:* $x = -27$, $y = -7$, $z = 30$; *right:* $x = 27$, $y = -7$, $z = 30$, each region of interest had a 10-mm radius). Before extracting the white matter time series, an exclusive mask was performed with the grey matter segmented image from each subject to eliminate voxels containing grey matter. A soft tissue mask of the facial and scalp soft tissues was used as previously described (Anderson *et al.*, 2011*c*). The mean soft tissue, CSF and white matter time series were then used as regressors in a general linear model (glmfit.m in MATLAB Statistics Toolbox) for the BOLD time series at each voxel in the brain, and the best fit was subtracted from the voxel's time series data, producing the signal-corrected time series images. Each voxel's time series was bandpass filtered with a frequency window of 0.001–0.1 Hz (Cordes *et al.*, 2001) and linearly detrended to correct for scanner drift. No smoothing was performed. These images were used for subsequent analysis.

Region of interest selection

Regions of interest ($n = 7266$) were selected to form a lattice covering the grey matter. A grey matter restriction mask was obtained by selecting voxels at $3 \times 3 \times 3$ mm resolution where the SPM8 grey.nii image showed intensity >0.3. Beginning with the right, inferior, posterior corner of the image, voxels were retained in the image if they were $\geqslant 5$ mm Euclidean distance from previously retained voxels. This yielded 7266 seed voxels, each separated by at least 5 mm. The grey matter restriction mask was then parcellated into 7266 regions of interest, based on which of the seed voxels was closest to any given voxel in the restriction mask. MNI coordinates of the 7266 seed voxels are tabulated in Supplementary Table 1. The resulting non-overlapping regions of interest averaged 4.9 ± 1.3 standard deviation (SD) voxels in size for 3 mm isotropic voxels.

For each subject, the post-processed BOLD time series was averaged from the voxels in each of the 7266 regions of interest. Pearson's correlation coefficients were calculated for each pair of voxels to obtain a 7266×7266 correlation matrix (26 393 745 connections per subject), and all correlation values were converted using Fisher *Z*-transformation (Lowe *et al.*, 1998; Kennedy and Courchesne, 2008*a*; Fox *et al.*, 2009; Murphy *et al.*, 2009).

Calculation of functional connectivity magnetic resonance imaging classification scores

A leave-one-out classifier was used to generate a classification score for each of the 40 autism and 40 control subjects. Each of the subjects in turn was excluded from the analysis, and for the remaining 79 subjects, the subset of connections for which the autism and control samples were significantly different in a two-tailed *t*-test for a specified *P*-value was identified. Because of the large number of connections, we attempted to exclude connections for which differences between autism and control samples were driven by an outlier. We therefore repeated this analysis after leaving out each of the remaining 79 subjects in turn, and retained connections that still differed between the two groups in a two-tailed *t*-test at the same specified *P*-value, no matter which additional subject was left out.

Once this subset of connections was identified for each left-out subject and each *P*-value tested, a classification score for the left-out-subject was calculated. For each connection in the subset, a linear fit was performed separately for autism and control samples from the 79 subjects remaining for that connection with subject age. An age-adjusted expected autism value and expected control value were determined by interpolating these best fit lines for the age of the subject that was left out. The Fisher-transformed correlation value for this connection for the left-out subject was then subtracted from

the expected autism value and the expected control value, and the difference was recorded. The mean of all such differences for the subset of connections tested was recorded as the functional connectivity MRI classification score for the left-out subject. A positive score indicated that the subject was more similar across the subset of connections to the remaining autism subjects; a negative score indicated the subject was more similar to the remaining control subjects. This entire procedure was repeated, leaving out each subject in turn, for all 26 393 745 connections in the dataset, as well as for subsets of connections selected by the *P*-values 0.001, 0.0001, 0.00 001 and 0.000 001.

Replication in an independent dataset of families

An optimum *P*-value of 0.001 was selected, and the subset of connections was identified to apply to a replication dataset. Each of the 80 subjects was left out in turn, and connections for which a two-tailed *t*-test was significant at uncorrected $P < 0.001$, no matter which subject was left out, was used for further analysis, yielding 58 908 connections.

The 21 subjects in the replication sample were scanned using identical procedures, with resting BOLD data processed in the same manner as above. An age-adjusted classification score was obtained in the same manner as described above for each of these 21 subjects compared with the 80 reference subjects. The same set of 58 908 connections described above was used for each of the 21 subjects.

Results

Classification scores for each of 40 autism and 40 typically developing subjects were calculated from a subset of the 26 393 745 connections between 7266 regions of interest. The subset was determined by a single *P*-value after leaving out one test subject at a time. A different set of connections was used for classification of each left-out subject, since defining the set of connections using all subjects could potentially introduce invalid bias.

Classification results for $P = 0.001$ are shown in Fig. 1A. A receiver operating characteristic (ROC) curve was calculated to estimate the ideal discriminant threshold, which was set at a functional connectivity MRI classification score of 0.008 (Fig. 1B). For this threshold, the classifier successfully predicted 30/40 control subjects (75%) and 33/40 autism subjects (83%), with a total accuracy of 63/80 (79%). To establish what results might be expected by chance from a binary classification algorithm, we evaluated a binomial distribution for 80 subjects. The probability of a 79% or better accuracy classification in 80 subjects based on random assignment is 1.13×10^{-7}. A two-tailed *t*-test of classification scores between autism and control samples was significantly different between the samples at $P = 1.6 \times 10^{-7}$. Classification was more accurate for younger subjects: for subjects <20 years of age, the classifier predicted 83% sensitivity (15/18 autism subjects), 95% specificity (18/19 control subjects) for 89% total accuracy (33/37, $P = 5.4 \times 10^{-7}$).

We applied this same classification algorithm with the same discriminant threshold to the independent replication sample, including eight individuals with an autism spectrum disorder and 13 unaffected siblings. The classifier performed at 75% sensitivity (6/8 autism spectrum disorder subjects), 69% specificity (9/13 control subjects) and 71% total accuracy ($P = 0.039$, Fig. 1C). The classifier again performed better on subjects <20 of age, with 83% sensitivity (5/6 autism spectrum disorder subjects), 100% specificity (5/5 control subjects) and 91% total accuracy ($P = 0.006$).

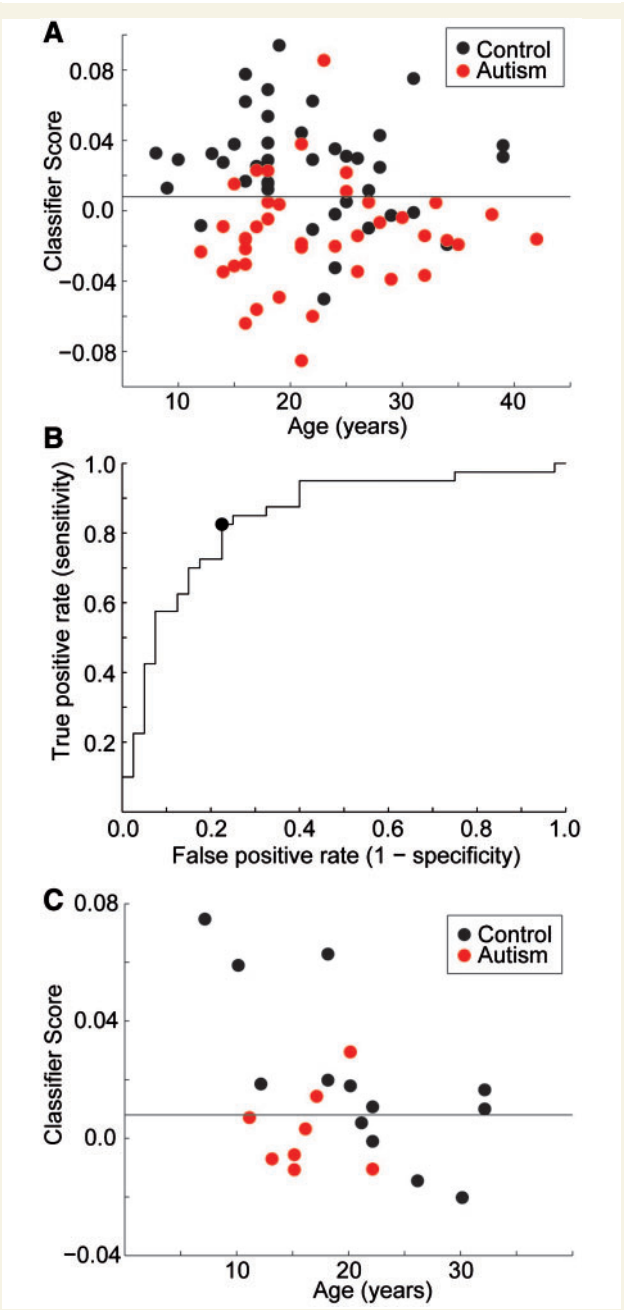

Figure 1 Accuracy of the leave-one-out classifier in the training dataset and replication in an independent sample of families. (**A**) Scatter plot showing classification scores for leave-one-out classifier in the training dataset for connections selected by $P < 0.001$. (**B**) Receiver operating characteristic (ROC) curve showing the optimal compromise between the true positive rate and false positive rate that was the basis for the discriminant threshold. (**C**) Scatter plot showing classification in the replication sample.

There is an inherent trade-off in using more connections in the classifier, which mitigates the noise in individual measurements, and using connections more specifically abnormal in autism. To evaluate an optimal number of connections, we performed classification separately using all 26.4 million connections, and using a *P*-value for connection selection ranging from 0.001 to 0.000 001. Results shown in Fig. 2 were calculated with the optimal discriminant threshold specific for each *P*-value.

Using all connections, specificity performed only at chance, indicating that the classifier was unable to reliably detect control subjects. Regardless of the discriminant threshold used, accuracy was lower than for any of the classifiers using a more specific subset of connections. Classification using a *P*-value of 0.001 and 0.0001 yielded equivalent sensitivity, specificity and accuracy. For $P = 0.001$, a mean of 89 411 $\pm$ 5389 SD connections was used to classify each subject.

The set of connections that was used for classifying the replication sample included 58 908 connections, obtained from the set of all connections satisfying $P < 0.001$ between remaining autism and control subjects no matter which two subjects were left out. If only one subject was left out, there were 91 851 connections satisfying $P < 0.001$ for remaining subjects. For connections that no longer satisfied $P < 0.001$ when a second subject was left out, these subjects were equally distributed between autism (50.5%) and control (49.5%) groups, with no significant difference in the frequency of 'outliers' between the two groups ($P = 0.85$). The set of 58 908 connections obtained from leaving out any two subjects was considered the subset of most informative connections in subsequent analyses. For $P = 0.0001$, an average of 15 976 $\pm$ 1409 connections was used for classification. For $P = 0.00\,001$, an average of 2535 $\pm$ 357 connections was used. For $P = 0.000\,001$, an average of 340 $\pm$ 67 connections was used.

The set of 58 908 most informative connections showed preferential involvement of specific brain regions, illustrated in Fig. 3. To evaluate whether some regions were significantly more represented in the set of informative connections, we considered a null hypothesis that all regions would be equally likely to be involved and performed permutation testing. By randomly assigning regions to 10 000 sets of 58 908 connections, we evaluated how many individual unordered pairs within the set of connections could contain the region as one of the two elements of the pair. For 95% of the 10 000 trials, no region was represented >33 times, so we took this as our threshold for significant overrepresentation in the sample. The brain regions that were disproportionately represented in the informative sample included regions of the bilateral fusiform gyrus, default mode network (posterior cingulate, medial prefrontal, bilateral temporoparietal junction, bilateral inferior temporal), bilateral anterior insula, bilateral superior parietal lobule and right orbitofrontal cortex.

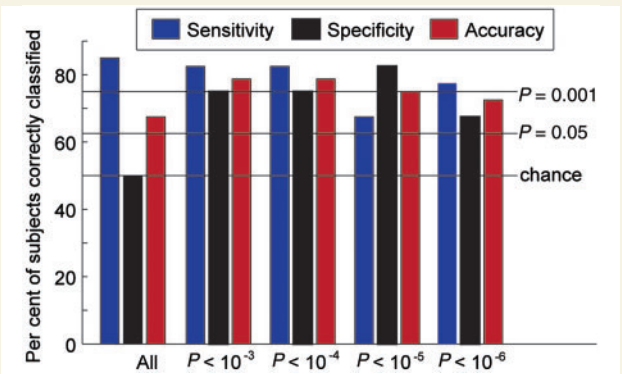

Figure 2 Dependence of classification accuracy on the subset of connections used. Sensitivity, specificity and total accuracy for the classifier is shown for all connections and for the subset of connections selected by a two-tailed *t*-test with *P*-values 0.001, 0.0001, 0.00 001 and 0.000 001. Horizontal lines show what per cent of subjects out of 40 would need to be classified correctly to achieve the specified *P*-value, and apply to sensitivity and specificity bars only.

A high spatial resolution array of connections allows the opportunity to cluster connections based on features such as connection length and strength to determine if specific types of connections (correlated, anticorrelated, long, short) inform the classifier differently with respect to autism and control samples. For connection strength, we used the mean Fisher-transformed correlation across all 80 subjects and grouped connections into 45 bins of 0.05, ranging from -0.35 to 1.85. For Euclidean distance between the centroids of the regions of interest, we measured distance in millimetres, acknowledging that this is only an approximate metric of connection distance, given that two regions of interest close together in contralateral occipital lobe, for example, may in fact be a much longer connection than the metric would indicate. Connections were binned into 32 bins of 5 mm, ranging from 10 to 165 mm.

Figure 4A shows the mean *t*-score between autism and control subjects for connections within each 2D bin. The distribution showed a clear topological pattern, with most negative *t*-statistics in the most positively correlated connections ranging from 10 to 150 mm distance (blue region). In contrast, mean *t*-scores were positive (indicating higher correlation values in autism) for negatively correlated sets of connections, particularly for long connections.

We evaluated the per cent of all connections in Fig. 4B that were included in the 58 908 subset of most informative connections to the classifier, and found that the red and orange shaded area from 50 to 100 mm between the regions of interest and with Fisher-transformed correlation values >0.5 were overwhelmingly the most informative to the classifier. A secondary peak, however, included connections where subjects with autism had greater correlation. This is equivalent to less anticorrelation for negatively correlated connections, since most of these connections were either negatively correlated or on the negative end of the distribution. The distributions between informative connections that showed higher versus lower correlation in autism were markedly different as a function both of path length and correlation strength (Fig. 4C and D).

To determine the extent to which our classification measurements corresponded to phenotypic properties of the samples, we correlated the functional connectivity MRI classification scores with verbal IQ, performance IQ, Social Responsiveness Scale, ADOS-G (social + communication) and ADI-R (communication) shown in Fig. 5. The classification scores in control subjects were not significantly correlated to any of the phenotypic

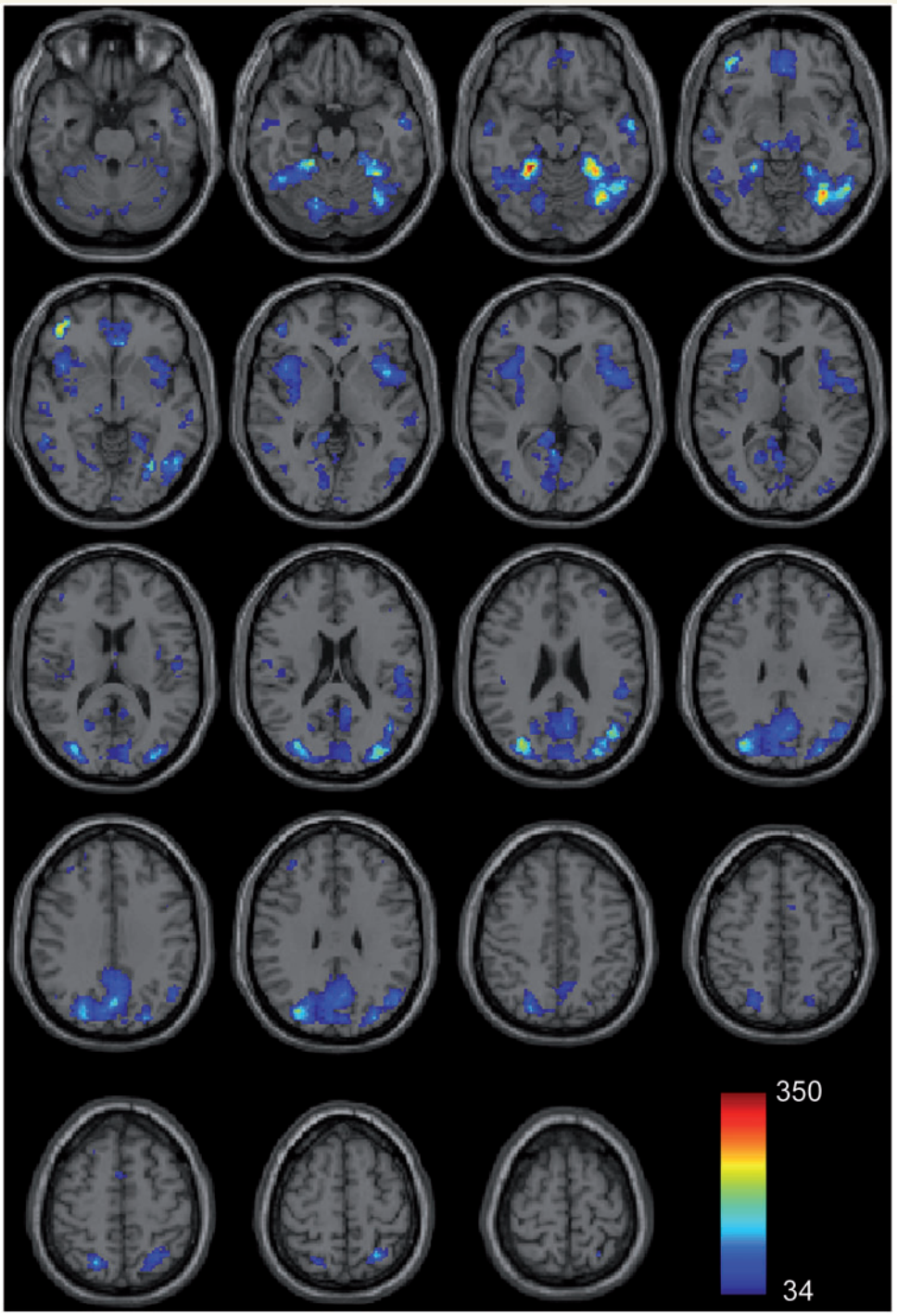

Figure 3 Brain regions most informative for classification. Shaded regions represent regions of interest disproportionately represented among informative connections, with colour scale representing the number of occurrences of the region of interest among the 58 908 most informative connections. Permutation testing demonstrated that if connections were randomly selected from the regions of interest, no region would be represented >33 times in 95% of simulations.

measurements. But in autism subjects, Social Responsiveness Scale, verbal IQ and ADOS-G's combined social and communication subscores were significantly correlated with the classification scores. Lower classification scores (more easily classified as autism) were associated with lower verbal IQ, higher Social Responsiveness Scale and higher ADOS-G scores (greater social impairment and disease severity). ADI-R also showed negative correlation with the classification score (more abnormal ADI-R values were more easily classified as autism) for each of the three ADI-R subtests, although none of these results achieved statistical

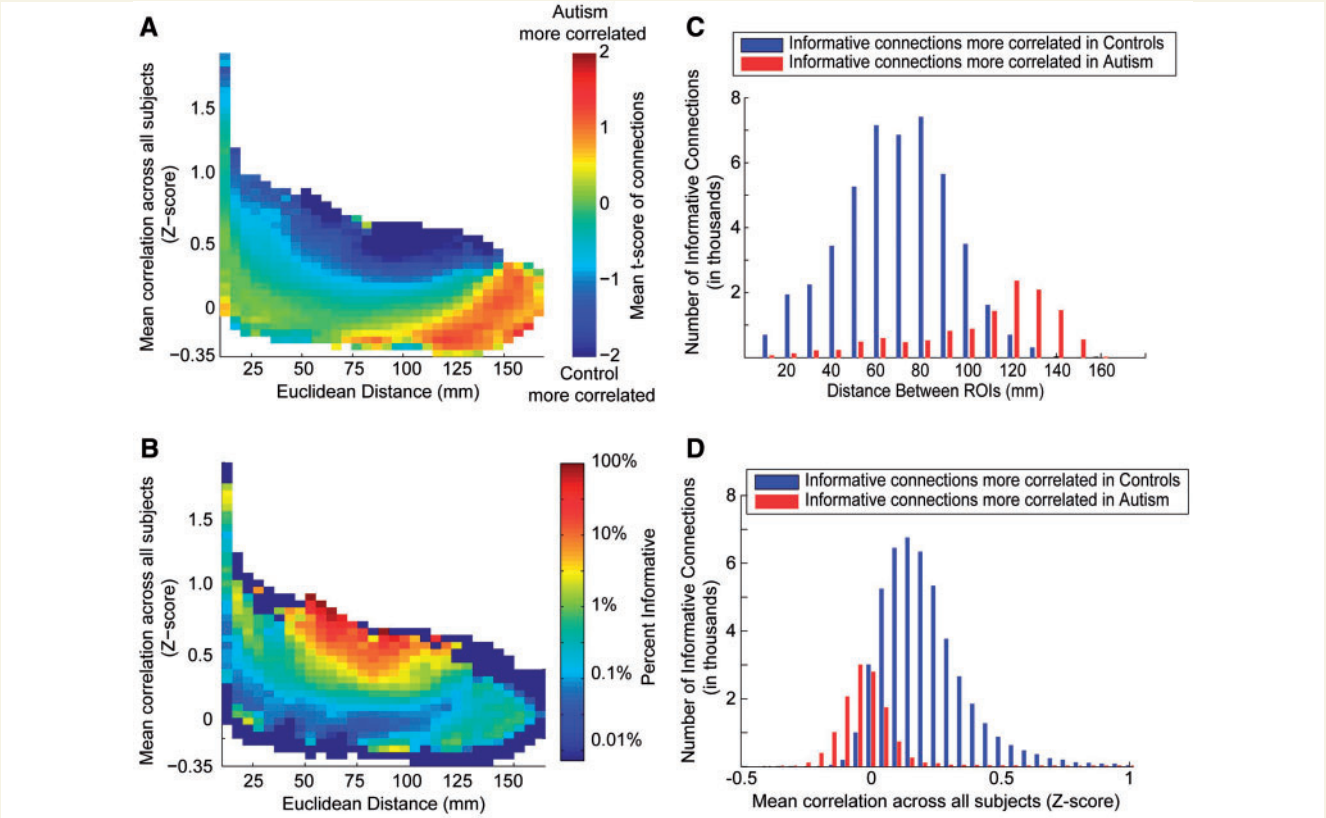

Figure 4 Connectivity differences in autism related to distance between brain regions and strength of correlation. (**A**) All connections were grouped into bins based on the distance in millimetre between the regions of interest (ROIs) versus the mean Fisher-transformed correlation across all 80 subjects. Within each bin, the two-tailed, two-sample *t*-score comparing autism and control subjects was averaged across the connections in the bin. Negative correlations were higher in subjects with autism (less anticorrelated), particularly between more distant regions. Strong positive correlations between brain regions were higher in control subjects. (**B**) Per cent of connections within each bin that were among the 58 908 most informative. (**C**) Distribution of informative connections with a positive versus negative *t*-score as a function of mean Fisher-transformed correlation across all subjects. (**D**) Distribution of informative connections with a positive versus negative *t*-score as a function of Euclidean distance.

significance (ADI-R social: $r = -0.13$, $P = 0.41$; ADI-R communication $r = -0.22$, $P = 0.14$; ADI-R repetitive and stereotyped behaviours $r = -0.12$, $P = 0.45$).

Discussion

We present data from a high spatial resolution array of connectivity measurements that can distinguish subjects with autism from typically developing controls with relatively high sensitivity and specificity. Classification accuracy was replicated in an independent dataset by distinguishing individuals with an autism spectrum disorder from their unaffected siblings. Datasets from families with affected and unaffected siblings were chosen for replication because this cohort may be a more realistic clinical diagnostic population, and because it could provide information on whether connectivity abnormalities in autism are shared by unaffected family members. This data-driven approach to classification yielded subsets of connections that were most informative in distinguishing autism and control subjects, and allowed characterization of whole-brain patterns of abnormal connectivity in autism that may inform pathophysiology, genetic and molecular mechanisms for autism, and the neural basis for clinical heterogeneity in autism.

Spatial distribution of abnormal connectivity

A survey of the most informative connections to the classifier identified a spatially heterogeneous distribution of abnormal connectivity. Brain regions that were significantly over-represented among abnormal connections in autism included the default mode network, superior parietal lobule, anterior insula and fusiform gyrus. Previous studies have identified abnormal connectivity within the default mode network in autism (Kennedy *et al.*, 2006; Kennedy and Courchesne, 2008*a*, *b*; Lombardo *et al.*, 2009; Monk *et al.*, 2009; Weng *et al.*, 2009; Assaf *et al.*, 2010). Task-based approaches have also identified abnormal function of the default mode network in autism, with failure to deactivate during attentionally demanding tasks (Kennedy *et al.*, 2006). Abnormal connectivity involving the superior parietal lobule, particularly along the intraparietal sulcus and anterior superior insula

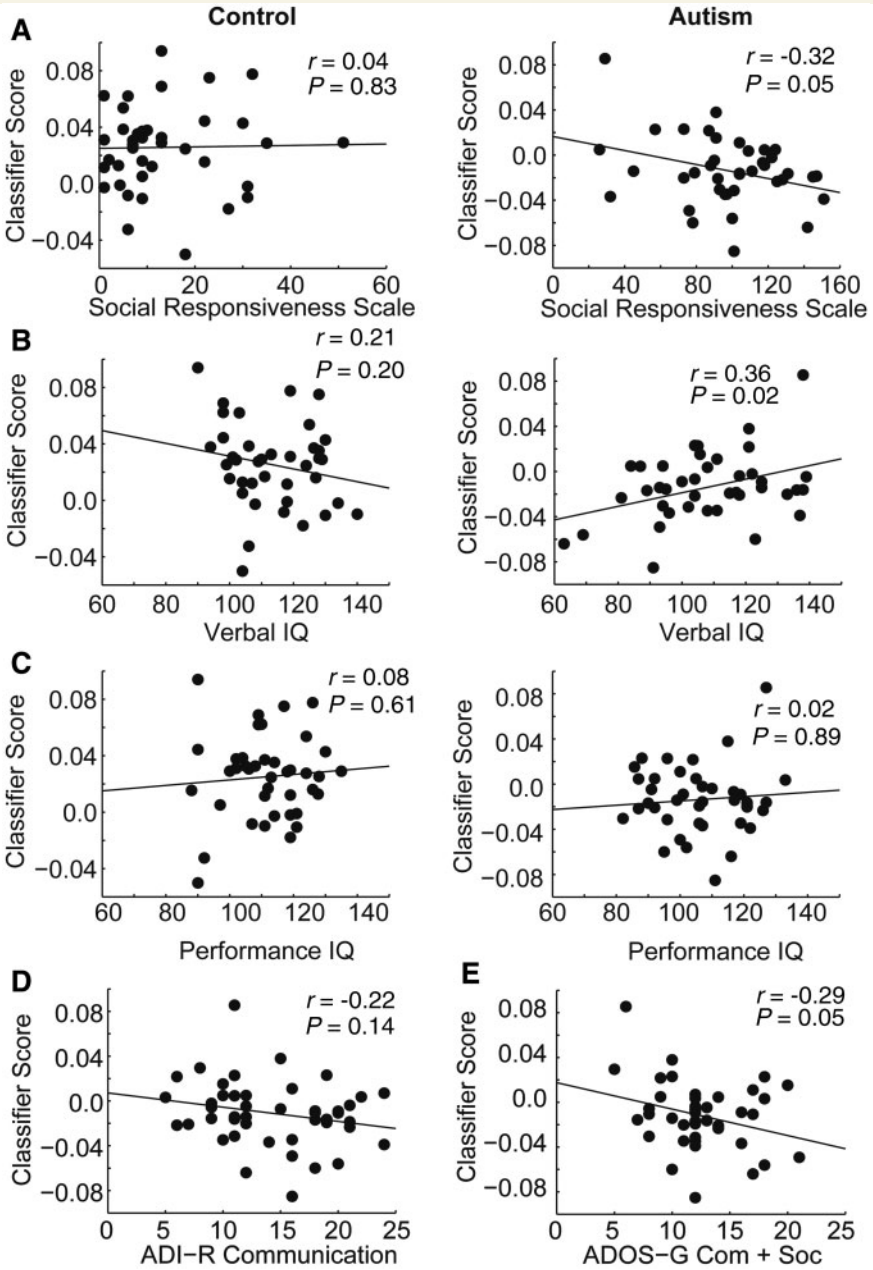

Figure 5 Relationship between functional connectivity classification score and clinical covariates. Scatter plots and best linear fit are shown for functional connectivity MRI classification score as a function of (**A**) Social Responsiveness Scale, (**B**) verbal IQ, (**C**) performance IQ, (**D**) ADI-R, (**E**) ADOS-G (social + communication) in autism and control samples. Significant relationships are annotated by correlation values and *P*-values above the plots.

as we observe, may also represent disordered connectivity within the attention control network.

Given a hypothesis where the default mode and attention control networks may compete for attentional resources between internal and external stimuli (Fox *et al.*, 2005), our findings and those in the studies above may be consistent with a phenotypic pattern of impaired communication within and between the default mode and attention control networks. This would be consistent with a clinical pattern wherein internal dialogue and narrative associated with activity in the default mode network (Gusnard *et al.*, 2001; Mason *et al.*, 2007; Troiani *et al.*, 2008; Wilson *et al.*, 2008; Yarkoni *et al.*, 2008; Whitney *et al.*, 2009) may be interrupted by intrusive external stimuli by failure to inhibit the attention control network. Alternately, attention to external stimuli associated with activity in the attention control network (Corbetta and Shulman, 2002; Fox *et al.*, 2005, 2006; Anderson *et al.*, 2010) may be abnormally interrupted by internal dialogue by a failure to adequately suppress the default mode network.

The anterior insulae are among the most consistently identified brain regions associated with social processing networks and have

demonstrated consistent hypoactivity in task-related functional MRI studies in autism (Uddin and Menon, 2009). The anterior superior insula is also a core component of the novelty detection or salience network involved in identification of novel or relevant stimuli across sensory modalities (Seeley *et al.*, 2007). The left frontoinsular region was specifically hypoactive in subjects with autism in a study of novelty detection using an auditory oddball paradigm (Gomot *et al.*, 2006).

The fusiform gyrus has also been the subject of previously identified abnormality in brain imaging studies of autism (Pierce and Redcay, 2008; Corbett *et al.*, 2009). Decreased functional connectivity of the fusiform gyrus to frontal regions has been reported in autism during facial processing tasks (Kleinhans *et al.*, 2008; Koshino *et al.*, 2008). A post-mortem study showed decreased numbers of neurons specifically in the fusiform gyrus in autism (van Kooten *et al.*, 2008).

Inter-region of interest distance and abnormal connectivity

Multiple prior reports have presented findings in support of a model of long-range underconnectivity and short-range overconnectivity in autism (Casanova and Trippe, 2009), yet functional connectivity studies have not previously defined 'long-range' or 'short-range' in terms of path length. A study of regional homogeneity in autism, where a voxel is compared with its immediate neighbours, showed decreased temporal correlation in autism (Paakki *et al.*, 2010) in most brain regions known to be abnormal in autism, although a few regions showed increased regional homogeneity. Our data indicate that positively correlated connections, even among the most short-range connections we measured, only 1–2 cm distant and presumably mediated by cortical U-fibres or short-range horizontal connections, already exhibit decreased connectivity in autism. Although we do not evaluate the hypothesis of local overconnectivity directly, our data constrain such local overconnectivity to subcentimetre spatial scales. It has been proposed that very short-range overconnectivity (or underconnectivity), by disrupting local network entropy and information capacity, may lead to long-range underconnectivity during development in autism (Belmonte *et al.*, 2004*b*). Such a hypothesis would be most consistent with our data if overconnectivity due to impaired synaptic pruning was at the columnar level, rather than at longer spatial extents by U-fibres or inter-regional cortico-cortical connections.

The only connections we observed that measured systematically higher in functional connectivity in autism were predominantly negatively correlated connections, particularly long-distance negative correlations. As such, it is possible that these connections also represent 'underconnectivity' in autism, but of long-range inhibitory connections. By utilizing a high spatial resolution array of connections, our data are less susceptible to averaging of positively and negatively correlated connections between larger regions of interest or networks that may represent a source for disagreement in the literature about a general underconnectivity theory of autism (Muller *et al.*, 2011).

Connection strength and abnormal connectivity

We also observed characteristic patterns in the distribution of strength of correlation between brain regions, and differences between autism and control samples. Specifically, we found that the most informative connections in distinguishing the samples were in the most strongly correlated brain regions. This may represent a bias towards connections that correspond to anatomic monosynaptic pathways, for which measurements of functional connectivity may be more precise or less influenced by shared inputs from other sources or indirect multisynaptic pathways that could combine excitatory and inhibitory components.

Phenotypic correlation of abnormal connectivity

Functional MRI classification scores were significantly correlated in subjects with autism, but not control subjects, to verbal IQ, ADOS (social + communication) and Social Responsiveness Scale measurements. For individuals with autism, these measurements are particularly instructive because they correspond to core diagnostic and phenotypic abnormalities in autism, verbal language impairment and abnormal social interaction. Other studies have also found connections between phenotypic metrics and functional connectivity in autism, for example, in a study of cingulo-insular connectivity (Di Martino *et al.*, 2009) and a study of visual attention (Belmonte *et al.*, 2010), which also found that unaffected siblings showed connectivity patterns that resembled control subjects rather than affected siblings, consistent with our results. The correlation of disease severity and functional connectivity indicates that connectivity abnormalities may be directly involved in the pathophysiology.

Methodological considerations

A recent meta-analysis of functional connectivity studies in autism identified widely heterogeneous methodological details that may underlie differing results obtained by the studies (Muller *et al.*, 2011). Methodological details were also mentioned by Jones *et al.* (2010) particularly related to global signal regression as a possible source of divergent results. The widespread use of regressing the global signal from the time series at each voxel prior to measuring functional connectivity (Fox *et al.*, 2009; Murphy *et al.*, 2009) has been shown to improve anatomic specificity of functional connections by mitigating physiological noise, but also introduces large anticorrelations. This has been shown to be related to subtracting components of large distributed networks from voxels to the extent that the voxel itself is in a large network (Anderson *et al.*, 2011*c*). This is problematic for studies involving neurodevelopmental or neuropathological groups, because spatially heterogeneous differences in connectivity are distributed to other brain regions, possibly limiting specificity. Particularly when evaluating large numbers of connections, the use of global signal regression may complicate attempts to resolve differences in specific types of connections and their relationship to disease pathophysiology. Therefore, we have used only regression to regions of interest in the white matter, CSF and facial soft tissues, and only

after excluding any grey matter voxels in proximity to the regions from which regressors were obtained (Anderson *et al.*, 2011*c*). We also did not detect any systematic differences in group head motion between our subjects with autism and control samples.

Study limitations

Further study will be necessary to assess how well the classifier we propose will generalize to younger ages (younger than 8 for controls and younger than 12 for autism spectrum disorder), cognitively lower functioning children and data collected across sites or with different scan sequence parameters. Nevertheless, it is reassuring that our classifier performed better for subjects <20 years of age, suggesting that younger age ranges may have more salient differences between autism and control subjects. Moreover, a recent study has found abnormal interhemispheric connectivity even in sleep for subjects as young as toddlers, suggesting that extension to very young ages may be possible (Dinstein *et al.*, 2011). We note that the broad age range used in the study may limit generalizability as well, and a larger sample of age-specific training datasets may serve to improve accuracy of the classifier, particularly in younger age ranges where connectivity is evolving through childhood and adolescence (Fair *et al.*, 2007). The classifier needs to be developed to better distinguish individuals with autism spectrum disorder from typically developing individuals, provide more useful information than diagnosis alone and very important for clinical utility, discriminate individuals with autism from patients with other developmental and neuropsychiatric disorders (Lainhart and Lange, 2011). In our results, unaffected family members were classified similarly to other control subjects, which might limit the utility of functional connectivity MRI classification in identifying intermediate phenotypes.

Accurate image-based diagnosis may be enhanced by combining this technique with multimodal classification schemes that involve diffusion tensor imaging (Lange *et al.*, 2010), structural imaging (Ecker *et al.*, 2010*a*, *b*; Jiao *et al.*, 2010) and neurophysiological measurements that by themselves show quite good autism classification ability. Longer BOLD imaging times may also improve diagnostic accuracy (Anderson *et al.*, 2011*a*, *d*). Given the large number of connections studied, each with considerable measurement noise, a larger training database will likely increase accuracy as well. Finally, we note that Euclidean distance is a poor substitute for more accurate path length measurements, and many of the connections tested may not correspond to monosynaptic pathways or well-defined anatomic circuits. Future studies might clarify whether more accurate path length measurements for connections such as that may be obtained with diffusion tensor tractography and restricting connections to those with plausible anatomic substrates may improve accuracy of the classifier.

Conclusion

Diagnostic accuracy of a functional connectivity MRI classification algorithm was 79% in a training dataset of individuals with autism and typically developing controls and 71% in a replication dataset of individuals with autism and their unaffected siblings, and classification scores were correlated with measures of verbal and social impairment in autism subjects. For subjects <20 years of age, accuracy improved to 89% in the training dataset and 91% in the replication dataset. Informative connections were seen in areas of the default mode network, anterior insula, fusiform gyrus and superior parietal lobule, all loci consistently found to be abnormal in imaging studies of autism. Most informative connections were between brain regions with highest correlation, with a smaller number of negatively correlated connections where subjects with autism had higher correlation (less anticorrelation), especially for long-range connections. These findings are consistent with a general underconnectivity theory of autism, including weaker long-range inhibitory connections.

Acknowledgements

The authors appreciate the assistance of Melody Johnson and Henry Buswell, of the University of Utah Centre for Advanced Imaging Research, for technical assistance in data acquisition. They acknowledge Drs William McMahon, Judith Miller, Mikle South and Nicanor Garcia, and past members of the Utah Autism Research Program. They also thank Barbara Young and Celeste Knoles of the Utah Autism Research Program, and express their sincere gratitude to the young people and their families who participated in the study. The content is solely the responsibility of the authors and does not necessarily represent the official views of the National Institute of Mental Health, National Institute of Neurological Disorders and Stroke, National Institute on Deafness and Other Communication Disorders or the National Institutes of Health.

Funding

National Institutes of Health (grant numbers K08 MH092697, RO1MH080826, P50MH60450, T32DC008553, R01NS34783); Autism Speaks Mentor-based Predoctoral Fellowship (grant number 1677); University of Utah Multidisciplinary Research Seed Grant; NRSA Predoctoral Fellowship (grant number F31 DC010143); Ben B. and Iris M. Margolis Foundation.

Supplementary Material

Supplementary material is available at *Brain* online.

References

Alexander AL, Lee JE, Lazar M, Boudos R, DuBray MB, Oakes TR, et al. Diffusion tensor imaging of the corpus callosum in Autism. Neuroimage 2007; 34: 61–73.

American Psychiatric Association. Diagnostic and Statistical Manual of Mental Disorders: DSM-IV, 4th edn. Washington, DC: American Psychiatric Association; 1994.

Anderson JS, Dhatt HS, Ferguson MA, Lopez-Larson M, Schrock L, House P, et al. Functional connectivity targeting for deep brain stimulation in essential tremor. AJNR Am J Neuroradiol 2011a. Advance Access published on September 1, 2011, doi:10.3174/ajnr.A2638.

Anderson JS, Druzgal TJ, Froehlich A, DuBray MB, Lange N, Alexander AL, et al. Decreased interhemispheric functional connectivity in autism. Cereb Cortex 2011b; 21: 1134–46.

Anderson JS, Druzgal TJ, Lopez-Larson M, Jeong EK, Desai K, Yurgelun-Todd D. Network anticorrelations, global regression, and phase-shifted soft tissue correction. Hum Brain Mapp 2011c; 32: 919–34.

Anderson JS, Ferguson MA, Lopez-Larson M, Yurgelun-Todd D. Reproducibility of single-subject functional connectivity measurements. AJNR Am J Neuroradiol 2011d; 32: 548–55.

Anderson JS, Ferguson MA, Lopez-Larson M, Yurgelun-Todd D. Topographic maps of multisensory attention. Proc Natl Acad Sci USA 2010; 107: 20110–4.

Assaf M, Jagannathan K, Calhoun VD, Miller L, Stevens MC, Sahl R, et al. Abnormal functional connectivity of default mode sub-networks in autism spectrum disorder patients. Neuroimage 2010; 53: 247–56.

Belmonte MK, Allen G, Beckel-Mitchener A, Boulanger LM, Carper RA, Webb SJ. Autism and abnormal development of brain connectivity. J Neurosci 2004a; 24: 9228–31.

Belmonte MK, Cook EH Jr, Anderson GM, Rubenstein JL, Greenough WT, Beckel-Mitchener A, et al. Autism as a disorder of neural information processing: directions for research and targets for therapy. Mol Psychiatry 2004b; 9: 646–63.

Belmonte MK, Gomot M, Baron-Cohen S. Visual attention in autism families: 'unaffected' sibs share atypical frontal activation. J Child Psychol Psychiatry 2010; 51: 259–76.

Brito AR, Vasconcelos MM, Domingues RC, Hygino da Cruz LC Jr, Rodrigues Lde S, Gasparetto EL, et al. Diffusion tensor imaging findings in school-aged autistic children. J Neuroimaging 2009; 19: 337–43.

Brock J, Brown CC, Boucher J, Rippon G. The temporal binding deficit hypothesis of autism. Dev Psychopathol 2002; 14: 209–24.

Casanova MF, El-Baz A, Mott M, Mannheim G, Hassan H, Fahmi R, et al. Reduced gyral window and corpus callosum size in autism: possible macroscopic correlates of a minicolumnopathy. J Autism Dev Disord 2009; 39: 751–64.

Casanova M, Trippe J. Radial cytoarchitecture and patterns of cortical connectivity in autism. Philos Trans R Soc Lond B Biol Sci 2009; 364: 1433–6.

Chen G, Ward BD, Xie C, Li W, Wu Z, Jones JL, et al. Classification of Alzheimer disease, mild cognitive impairment, and normal cognitive status with large-scale network analysis based on resting-state functional MR imaging. Radiology 2011; 259: 213–21.

Cherkassky VL, Kana RK, Keller TA, Just MA. Functional connectivity in a baseline resting-state network in autism. Neuroreport 2006; 17: 1687–90.

Cheung C, Chua SE, Cheung V, Khong PL, Tai KS, Wong TK, et al. White matter fractional anisotrophy differences and correlates of diagnostic symptoms in autism. J Child Psychol Psychiatry 2009; 50: 1102–12.

Constantino JN, Todd RD. Autistic traits in the general population: a twin study. Arch Gen Psychiatry 2003; 60: 524–30.

Corbett BA, Carmean V, Ravizza S, Wendelken C, Henry ML, Carter C, et al. A functional and structural study of emotion and face processing in children with autism. Psychiatry Res 2009; 173: 196–205.

Corbetta M, Shulman GL. Control of goal-directed and stimulus-driven attention in the brain. Nat Rev Neurosci 2002; 3: 201–15.

Cordes D, Haughton VM, Arfanakis K, Carew JD, Turski PA, Moritz CH, et al. Frequencies contributing to functional connectivity in the cerebral cortex in "resting-state" data. AJNR Am J Neuroradiol 2001; 22: 1326–33.

Courchesne E, Pierce K. Why the frontal cortex in autism might be talking only to itself: local over-connectivity but long-distance disconnection. Curr Opin Neurobiol 2005; 15: 225–30.

Damarla SR, Keller TA, Kana RK, Cherkassky VL, Williams DL, Minshew NJ, et al. Cortical underconnectivity coupled with preserved visuospatial cognition in autism: evidence from an fMRI study of an embedded figures task. Autism Res 2010; 3: 273–9.

Di Martino A, Scheres A, Margulies DS, Kelly AM, Uddin LQ, Shehzad Z, et al. Functional connectivity of human striatum: a resting state fMRI Study. Cereb Cortex 2008; 18: 2735–47.

Di Martino A, Shehzad Z, Kelly C, Roy AK, Gee DG, Uddin LQ, et al. Relationship between cingulo-insular functional connectivity and autistic traits in neurotypical adults. Am J Psychiatry 2009; 166: 891–9.

Dinstein I, Pierce K, Eyler L, Solso S, Malach R, Behrmann M, et al. Disrupted neural synchronization in toddlers with autism. Neuron 2011; 70: 1218–25.

Dosenbach NU, Nardos B, Cohen AL, Fair DA, Power JD, Church JA, et al. Prediction of individual brain maturity using fMRI. Science 2010; 329: 1358–61.

Duvall JA, Lu A, Cantor RM, Todd RD, Constantino JN, Geschwind DH. A quantitative trait locus analysis of social responsiveness in multiplex autism families. Am J Psychiatry 2007; 164: 656–62.

Ecker C, Marquand A, Mourao-Miranda J, Johnston P, Daly EM, Brammer MJ, et al. Describing the brain in autism in five dimensions–magnetic resonance imaging-assisted diagnosis of autism spectrum disorder using a multiparameter classification approach. J Neurosci 2010a; 30: 10612–23.

Ecker C, Rocha-Rego V, Johnston P, Mourao-Miranda J, Marquand A, Daly EM, et al. Investigating the predictive value of whole-brain structural MR scans in autism: a pattern classification approach. Neuroimage 2010b; 49: 44–56.

Elliott CD. Differntial Ability Scales-II (DAS-II). San Antonio: The Psychological Corporation; 1990.

Fair DA, Dosenbach NU, Church JA, Cohen AL, Brahmbhatt S, Miezin FM, et al. Development of distinct control networks through segregation and integration. Proc Natl Acad Sci USA 2007; 104: 13507–12.

Fletcher PT, Whitaker RT, Tao R, DuBray MB, Froehlich A, Ravichandran C, et al. Microstructural connectivity of the arcuate fasciculus in adolescents with high-functioning autism. Neuroimage 2010; 51: 1117–25.

Fox MD, Corbetta M, Snyder AZ, Vincent JL, Raichle ME. Spontaneous neuronal activity distinguishes human dorsal and ventral attention systems. Proc Natl Acad Sci USA 2006; 103: 10046–51.

Fox MD, Snyder AZ, Vincent JL, Corbetta M, Van Essen DC, Raichle ME. The human brain is intrinsically organized into dynamic, anticorrelated functional networks. Proc Natl Acad Sci USA 2005; 102: 9673–8.

Fox MD, Zhang D, Snyder AZ, Raichle ME. The global signal and observed anticorrelated resting state brain networks. J Neurophysiol 2009; 101: 3270–83.

Geschwind DH, Levitt P. Autism spectrum disorders: developmental disconnection syndromes. Curr Opin Neurobiol 2007; 17: 103–11.

Gomot M, Bernard FA, Davis MH, Belmonte MK, Ashwin C, Bullmore ET, et al. Change detection in children with autism: an auditory event-related fMRI study. Neuroimage 2006; 29: 475–84.

Gusnard DA, Akbudak E, Shulman GL, Raichle ME. Medial prefrontal cortex and self-referential mental activity: relation to a default mode of brain function. Proc Natl Acad Sci USA 2001; 98: 4259–64.

Hughes JR. Autism: the first firm finding = underconnectivity? Epilepsy Behav 2007; 11: 20–4.

Jiao Y, Chen R, Ke X, Chu K, Lu Z, Herskovits EH. Predictive models of autism spectrum disorder based on brain regional cortical thickness. Neuroimage 2010; 50: 589–99.

Jones TB, Bandettini PA, Kenworthy L, Case LK, Milleville SC, Martin A, et al. Sources of group differences in functional connectivity: an investigation applied to autism spectrum disorder. Neuroimage 2010; 9: 401–14.

Just MA, Cherkassky VL, Keller TA, Kana RK, Minshew NJ. Functional and anatomical cortical underconnectivity in autism: evidence from an FMRI study of an executive function task and corpus callosum morphometry. Cereb Cortex 2007; 17: 951–61.

Just MA, Cherkassky VL, Keller TA, Minshew NJ. Cortical activation and synchronization during sentence comprehension in high-functioning autism: evidence of underconnectivity. Brain 2004; 127 (Pt 8): 1811–21.

Kana RK, Keller TA, Cherkassky VL, Minshew NJ, Just MA. Sentence comprehension in autism: thinking in pictures with decreased functional connectivity. Brain 2006; 129 (Pt 9): 2484–93.
Kana RK, Keller TA, Cherkassky VL, Minshew NJ, Just MA. Atypical frontal-posterior synchronization of theory of mind regions in autism during mental state attribution. Soc Neurosci 2009; 4: 135–52.
Kana RK, Keller TA, Minshew NJ, Just MA. Inhibitory control in high-functioning autism: decreased activation and underconnectivity in inhibition networks. Biol Psychiatry 2007; 62: 198–206.
Kennedy DP, Courchesne E. The intrinsic functional organization of the brain is altered in autism. Neuroimage 2008a; 39: 1877–85.
Kennedy DP, Courchesne E. Functional abnormalities of the default network during self- and other-reflection in autism. Soc Cogn Affect Neurosci 2008b; 3: 177–90.
Kennedy DP, Redcay E, Courchesne E. Failing to deactivate: resting functional abnormalities in autism. Proc Natl Acad Sci USA 2006; 103: 8275–80.
Kleinhans NM, Richards T, Sterling L, Stegbauer KC, Mahurin R, Johnson LC, et al. Abnormal functional connectivity in autism spectrum disorders during face processing. Brain 2008; 131 (Pt 4): 1000–12.
Koshino H, Carpenter PA, Minshew NJ, Cherkassky VL, Keller TA, Just MA. Functional connectivity in an fMRI working memory task in high-functioning autism. Neuroimage 2005; 24: 810–21.
Koshino H, Kana RK, Keller TA, Cherkassky VL, Minshew NJ, Just MA. fMRI investigation of working memory for faces in autism: visual coding and underconnectivity with frontal areas. Cereb Cortex 2008; 18: 289–300.
Lainhart JE, Lange N. The biological broader autism phenotype. In: Amaral D, Geschwind D, Dawson G, editors. Autism spectrum disorders. New York: Oxford University Press; 2011.
Lange N, Dubray MB, Lee JE, Froimowitz MP, Froehlich A, Adluru N, et al. Atypical diffusion tensor hemispheric asymmetry in autism. Autism Res 2010; 3: 350–8.
Lee PS, Yerys BE, Della Rosa A, Foss-Feig J, Barnes KA, James JD, et al. Functional connectivity of the inferior frontal cortex changes with age in children with autism spectrum disorders: a fcMRI study of response inhibition. Cereb Cortex 2009; 19: 1787–94.
Leyfer OT, Folstein SE, Bacalman S, Davis NO, Dinh E, Morgan J, et al. Comorbid psychiatric disorders in children with autism: interview development and rates of disorders. J Autism Dev Disord 2006; 36: 849–61.
Lombardo MV, Chakrabarti B, Bullmore ET, Sadek SA, Pasco G, Wheelwright SJ, et al. Atypical neural self-representation in autism. Brain 2009; 133 (Pt 2): 611–24.
Lord C, Risi S, Lambrecht L, Cook EH Jr, Leventhal BL, DiLavore PC, et al. The autism diagnostic observation schedule-generic: a standard measure of social and communication deficits associated with the spectrum of autism. J Autism Dev Disord 2000; 30: 205–23.
Lord C, Rutter M, Le Couteur A. Autism diagnostic interview-revised: a revised version of a diagnostic interview for caregivers of individuals with possible pervasive developmental disorders. J Autism Dev Disord 1994; 24: 659–85.
Lowe MJ, Mock BJ, Sorenson JA. Functional connectivity in single and multislice echoplanar imaging using resting-state fluctuations. Neuroimage 1998; 7: 119–32.
Mason MF, Norton MI, Van Horn JD, Wegner DM, Grafton ST, Macrae CN. Wandering minds: the default network and stimulus-independent thought. Science 2007; 315: 393–5.
Mason RA, Williams DL, Kana RK, Minshew N, Just MA. Theory of mind disruption and recruitment of the right hemisphere during narrative comprehension in autism. Neuropsychologia 2008; 46: 269–80.
Monk CS, Peltier SJ, Wiggins JL, Weng SJ, Carrasco M, Risi S, et al. Abnormalities of intrinsic functional connectivity in autism spectrum disorders. Neuroimage 2009; 47: 764–72.
Mostofsky SH, Powell SK, Simmonds DJ, Goldberg MC, Caffo B, Pekar JJ. Decreased connectivity and cerebellar activity in autism during motor task performance. Brain 2009; 132: 2413–25.
Muller RA, Shih P, Keehn B, Deyoe JR, Leyden KM, Shukla DK. Underconnected, but How? A survey of functional connectivity MRI studies in autism spectrum disorders. Cereb Cortex 2011; 21: 2233–43.
Murphy K, Birn RM, Handwerker DA, Jones TB, Bandettini PA. The impact of global signal regression on resting state correlations: are anti-correlated networks introduced? Neuroimage 2009; 44: 893–905.
Oldfield RC. The assessment and analysis of handedness: the Edinburgh inventory. Neuropsychologia 1971; 9: 97–113.
Paakki JJ, Rahko J, Long XY, Moilanen I, Tervonen O, Nikkinen J, et al. Alterations in regional homogeneity of resting-state brain activity in autism spectrum disorders. Brain Res 2010; 1329: 169–79.
Pierce K, Redcay E. Fusiform function in children with an autism spectrum disorder is a matter of "who". Biol Psychiatry 2008; 64: 552–60.
Rippon G, Brock J, Brown C, Boucher J. Disordered connectivity in the autistic brain: challenges for the "new psychophysiology". Int J Psychophysiol 2007; 63: 164–72.
Seeley WW, Menon V, Schatzberg AF, Keller J, Glover GH, Kenna H, et al. Dissociable intrinsic connectivity networks for salience processing and executive control. J Neurosci 2007; 27: 2349–56.
Shehzad Z, Kelly AM, Reiss PT, Gee DG, Gotimer K, Uddin LQ, et al. The resting brain: unconstrained yet reliable. Cereb Cortex 2009; 19: 2209–29.
Shukla DK, Keehn B, Muller RA. Tract-specific analyses of diffusion tensor imaging show widespread white matter compromise in autism spectrum disorder. J Child Psychol Psychiatry 2010; 52: 286–95.
Shukla DK, Keehn B, Smylie DM, Muller RA. Microstructural abnormalities of short-distance white matter tracts in autism spectrum disorder. Neuropsychologia 2011; 49: 1378–82.
Troiani V, Fernandez-Seara MA, Wang Z, Detre JA, Ash S, Grossman M. Narrative speech production: an fMRI study using continuous arterial spin labeling. Neuroimage 2008; 40: 932–9.
Uddin LQ, Menon V. The anterior insula in autism: Under-connected and under-examined. Neurosci Biobehav Rev 2009; 33: 1198–203.
Van Dijk KR, Hedden T, Venkataraman A, Evans KC, Lazar SW, Buckner RL. Intrinsic functional connectivity as a tool for human connectomics: theory, properties, and optimization. J Neurophysiol 2010; 103: 297–321.
van Kooten IA, Palmen SJ, von Cappeln P, Steinbusch HW, Korr H, Heinsen H, et al. Neurons in the fusiform gyrus are fewer and smaller in autism. Brain 2008; 131 (Pt 4): 987–99.
Villalobos ME, Mizuno A, Dahl BC, Kemmotsu N, Muller RA. Reduced functional connectivity between V1 and inferior frontal cortex associated with visuomotor performance in autism. Neuroimage 2005; 25: 916–25.
Wechsler D. Wechsler Intelligence Scale for Children - Third Edition (WISC-III). San Antonio: The Psychological Corporation; 1991.
Wechsler D. Wechsler Adult Intelligence Scale - Third Edition (WAIS-III). San Antonio: The Psychological Corporation; 1997.
Wechsler D. Wechsler Abbreviated Scale of Intelligence (WASI). San Antonio: The Psychological Corporation; 1999.
Weng SJ, Wiggins JL, Peltier SJ, Carrasco M, Risi S, Lord C, et al. Alterations of resting state functional connectivity in the default network in adolescents with autism spectrum disorders. Brain Res 2009; 1313: 202–14.
Whitney C, Huber W, Klann J, Weis S, Krach S, Kircher T. Neural correlates of narrative shifts during auditory story comprehension. Neuroimage 2009; 47: 360–6.
Wilson SM, Molnar-Szakacs I, Iacoboni M. Beyond superior temporal cortex: intersubject correlations in narrative speech comprehension. Cereb Cortex 2008; 18: 230–42.
Yarkoni T, Speer NK, Zacks JM. Neural substrates of narrative comprehension and memory. Neuroimage 2008; 41: 1408–25.
Zuo XN, Kelly C, Adelstein JS, Klein DF, Castellanos FX, Milham MP. Reliable intrinsic connectivity networks: test-retest evaluation using ICA and dual regression approach. Neuroimage 2009; 49: 2163–77.